

1 **Pathogenicity test of *Vibrio parahaemolyticus* in Pacific white shrimp *Penaeus vannamei***

2 **Widanarni¹⁾, Badar Kautsar ¹⁾, Dinamella Wahjuningrum¹⁾, dan Muhamad Gustilatov^{1*)}**

3

4 ¹ Department of Aquaculture, Faculty of Fisheries and Marine Science, IPB University,

5

Indonesia 16680

6

7

*Corresponding author: mgustilatov@apps.ipb.ac.id

8

Raya Dramaga St. IPB Dramaga Campus, Bogor, Indonesia 16680

9

10

Received : 06 Sept 2024; Revised: 10 Oct 2024; Accepted: 10 Oct 2024

Accepted Manuscript

ABSTRACT

11
12
13
14
15
16
17
18
19
20
21
22
23
24
25
26
27
28
29
30
31
32
33
34

One of the common diseases affecting the Pacific white shrimp (*Penaeus vannamei*) culture is vibriosis, caused by infection with *Vibrio* species, including *Vibrio parahaemolyticus*. Certain strains of *V. parahaemolyticus* that carry the PirA and PirB toxins are responsible for causing acute hepatopancreatic necrosis disease (AHPND). This study aimed to assess the pathogenicity of *V. parahaemolyticus* in *P. vannamei* using bacterial isolates from different sources. A challenge test was conducted using *P. vannamei* with an average weight of 0.9 ± 0.1 g, exposed to bacterial concentrations of 10^4 CFU/mL, as determined by lethal concentration 50% (LC₅₀). The experiment followed a completely randomized design with three treatments and three replicates: a control group (K) of uninfected shrimp, shrimp infected with *V. parahaemolyticus* from Tasikmalaya, West Java (Vp-1), and shrimp infected with *V. parahaemolyticus* from Situbondo, East Java (Vp-2). Parameters observed included the confirmation of *V. parahaemolyticus* and AHPND via polymerase chain reaction (PCR), mortality rate, clinical symptoms, bacterial load, and immune response indicators, including total haemocyte count, phagocytic activity, respiratory burst, phenoloxidase activity, and histopathological examination of the hepatopancreas and intestines. Both Vp-1 and Vp-2 isolates were identified as *V. parahaemolyticus* AHPND strains, infecting shrimp with clinical signs such as pale hepatopancreas, empty intestines, and lethargic movement. Tissue damage, including extensive necrosis in the hepatopancreas and intestines, was observed, leading to mortality rates of 73.33-81.67% with an average time to death ranging from 24.28 to 65.44 hours postinfection.

Keywords: AHPND, histopathology, pathogenicity, shrimp, *V. parahaemolyticus*.

35 1. INTRODUCTION

36 The Pacific white shrimp (*Penaeus vannamei*) is a highly valuable aquaculture
37 commodity in both Indonesia and globally. In 2022, global production of white shrimp reached
38 6.8 million tons, making it the most produced aquaculture species, followed by *Crassostrea* spp.
39 and grass carp (FAO, 2022). Global production of white shrimp experienced significant growth
40 between 2010 and 2020, increasing by 3.2 million tons (FAO, 2022). In Indonesia, shrimp
41 production reached 881,599 tons (KKP, 2022), contributing approximately USD 2 billion to
42 global exports in 2019 (FAO, 2022). The advantages of white shrimp include rapid growth, short
43 production cycles, and high stocking densities.

44 However, increased shrimp production faces several challenges, one of which is
45 disease outbreaks. One of the most common diseases in shrimp farming is vibriosis,
46 caused by bacterial infections from *Vibrio* species, including *Vibrio parahaemolyticus*
47 (Aguirre-Guzman et al., 2010). Infections by *V. parahaemolyticus* can cause
48 abnormalities in shrimp, such as gill necrosis, lethargy, anorexia, and in acute conditions,
49 mortality rates can reach 100% (Abdel-latif et al., 2022).

50 Certain strains of *V. parahaemolyticus* that produce PirA and PirB toxins can
51 cause hepatopancreatic dysfunction, leading to Acute Hepatopancreatic Necrosis Disease
52 (AHPND) (Han et al., 2015). These toxins damage the hepatopancreas tissue of shrimp,
53 resulting in clinical symptoms that often lead to mass mortality in white shrimp. *V.*
54 *parahaemolyticus* infections cause substantial economic losses in the shrimp aquaculture
55 industry. The disease was first identified in China in 2009, referred to as Early Mortality
56 Syndrome (EMS) due to rapid mortality during the first month of cultivation, and has
57 since spread to several countries in Asia and the Americas (Hong et al., 2016;
58 Zorriehzahra & Banaederakhshan, 2015). Between 2009 and 2018, AHPND caused by *V.*
59 *parahaemolyticus* led to global economic losses amounting to USD 44 billion (Tang &

60 Bondad-Reantaso, 2019). Therefore, developing effective control and prevention
61 strategies is critical to protecting shrimp populations from AHPND.

62 Pathogenicity tests on *V. parahaemolyticus* in white shrimp are essential for
63 understanding how the bacteria cause infections in shrimp, thus aiding in the development
64 of more effective prevention and treatment strategies. These tests involve exposing
65 healthy shrimp to the test bacteria and monitoring infection symptoms, such as behavioral
66 changes, morphological damage, tissue necrosis, and mortality (Saulnier et al., 2000).

67 Pathogenicity tests can help shrimp farmers identify and control infections in
68 white shrimp, ultimately reducing the economic losses caused by *V. parahaemolyticus*.
69 This study aims to evaluate the pathogenicity of *V. parahaemolyticus* from different
70 bacterial isolate sources in white shrimp to compare the effects of isolate variation and its
71 relationship to pathogenicity in causing disease in shrimp.

72

73 **2. MATERIAL AND METHOD**

74 **2.1 Experimental Design**

75 This study employed a completely randomized design with three treatments, each
76 with three replicates. The treatments included: white shrimp uninfected by *Vibrio*
77 *parahaemolyticus* (K) as the control group, white shrimp infected with *V.*
78 *parahaemolyticus* isolated from Tasikmalaya, West Java (Vp-1), and white shrimp
79 infected with *V. parahaemolyticus* isolated from Situbondo, East Java (Vp-2).

80 **2.2 Bacterial Preparation**

81 The bacteria used in this study were *Vibrio parahaemolyticus* isolated from
82 Tasikmalaya, West Java, and Situbondo, East Java. *V. parahaemolyticus* was cultured on
83 thiosulfate citrate bile salt sucrose (TCBS) agar, with rifampicin (50 µg/mL) as an

84 antibiotic marker. Bacterial colonies grown on TCBS were then cultured in liquid sea
85 water complete (SWC) medium and incubated in a water bath shaker at 29°C with a
86 shaking speed of 130 rpm for 18-24 hours.

87 **2.3 Shrimp Maintenance and Challenge Test**

88 The white shrimp (*P. vannamei*) used in this study were sourced from the Specific
89 Pathogen Free (SPF)-certified hatchery of PT Syaqua, Anyer, Banten Province, with an
90 average body weight of 0.9±0.1 g. The shrimp were stocked at a density of 1 shrimp per
91 liter in aquariums measuring 60 cm x 40 cm x 35 cm, containing 20 L of water. They
92 were reared for seven days and fed commercial pellets containing 40% protein four times
93 a day, at 07:00, 12:00, 17:00, and 22:00. The challenge test was conducted using *Vibrio*
94 *parahaemolyticus* (10⁴ CFU/mL; based on LC₅₀ test) through an immersion method
95 starting at the beginning of the maintenance period (Widanarni *et al.* 2024). Water quality
96 parameters, including dissolved oxygen, pH, temperature, and salinity, were measured
97 with values ranging from 5.2-6.4 mg/L, 7.58-7.75, 28.1-29.5 °C, and 30-32 g/L,
98 respectively.

99 **2.4 Observation Parameters**

100 2.4.1 Confirmation of *V. parahaemolyticus* and AHPND

101 The characterization of *V. parahaemolyticus* was performed by culturing the
102 isolates on TCBS and CHROMagar media. Colony color and morphology were observed
103 and compared to reference characteristics for each medium. The confirmation of AHPND
104 in *V. parahaemolyticus* was conducted using the PCR method prior to the challenge test.
105 The PCR process included DNA extraction, amplification, and electrophoresis. Specific
106 primers used for AHPND confirmation were AP4 (targeting *pirA* and *pirB* genes). The
107 AP4 primer set for the first reaction (first-step PCR) was AP4-F1 (5'-ATG-AGT-AAC-

108 AAT-ATA-AAA-CAT-GAA-AC-3') and AP4-R1 (5'-ACG-ATT-TCG-ACG-TTC-
109 CCC-AA-3'), while for the second reaction (nested PCR), AP4-F2 (5'-TTG-AGA-ATA-
110 AGG-GAC-GTG-GG-3') and AP4-R2 (5'-GTT-AGT-CAT-GTG-AGC-ACC-TTC-3')
111 were used. The amplicon size indicating *V. parahaemolyticus* AHPND strain was 230 bp
112 (OIE 2019).

113 2.4.2 Mortality and Average Time of Death in White Shrimp

114 Shrimp mortality observations were made every 12 hours. Changes in the shrimp
115 death rate were monitored to determine the peak and lowest mortality times. Mortality
116 rate, one of the key parameters, indicates the percentage of dead shrimp from the initial
117 population. Mortality rates were observed after the maintenance period following
118 bacterial infection. Shrimp death numbers during the challenge test were used to assess
119 the pathogenicity of the bacteria. The time of death was recorded every 12 hours, starting
120 from the challenge test, and daily mortality was calculated using the formula from
121 Nitimulyo et al. (2005).

$$122 \text{ MTD} = \frac{\sum_{i=1}^n a_i b_i}{\sum_{i=1}^n b_i}$$

123 Notes:

124 MTD = Mean time to death

125 a = Time of death (hours)

126 b = Number of death shrimp (shrimp)

127 i = Summation index

128 n = Upper limit of summation

129 2.4.3 Total Bacterial Count

130 Bacterial population counts were conducted using the plate count method at the
131 beginning, middle, and end of the maintenance period. Observations included the

132 abundance of *V. parahaemolyticus* in the rearing water and shrimp body. The media used
133 were TCBS with rifampicin at 50 µg/mL and CHROMagar. Bacterial population
134 calculation was performed using the formula from Madigan et al. (2003) as follows:

$$135 \quad \text{Bacterial population (CF/mL)} = \sum \text{Colony} \times \frac{1}{\text{Dilution Factor}} \times \frac{1}{\text{Sample Volume (mL)}}$$

136 2.4.4. White Shrimp Immune Response

137 A total of 0.3 g of shrimp larvae in a mortar was added to 0.9 mL of anticoagulant
138 (1:3 w/v) and then gently ground until the larvae's bodies were crushed. The hemolymph-
139 anticoagulant mixture was pipetted and placed into a microtube and homogenized by
140 gently swirling in a figure-eight motion. The hemolymph-anticoagulant mixture was then
141 applied to a hemocytometer, and Total Hemocyte Count (THC) was directly counted
142 under a microscope at 100× magnification (Tampangallo et al. 2012). The THC was
143 calculated using the following formula:

$$144 \quad \text{THC} = \frac{\sum \text{Counted cells}}{\text{Grid volume}} \times \text{Dilution factor}$$

145 Hemolymph (0.1 mL) was placed in a microplate and evenly mixed with 25 µL
146 *Staphylococcus aureus* suspension in PBS (10^7 cells/mL), incubated at room temperature
147 for 20 minutes. A drop of the hemolymph-bacteria mixture (5–10 µL) was placed on a
148 glass slide, smeared, and air-dried. The smear was then fixed with 100% methanol for 5
149 minutes and air-dried. It was stained by immersing the slide in Giemsa stain for 15
150 minutes, rinsed with running water, and air-dried with tissue. The number of cells
151 undergoing phagocytosis out of 100 observed phagocytes was counted (Anderson and
152 Siwicki 1993).

$$153 \quad \text{AF (\%)} = \frac{\text{Number of Phagocytic Cells}}{\text{Number of Phagocytes}} \times 100$$

154 The respiratory burst activity of hemocytes was measured based on the reduction
155 of nitroblue tetrazolium (NBT), indicating superoxide anion (O₂⁻) production. A total of
156 250 µL of the hemolymph-anticoagulant mixture was incubated at room temperature for
157 30 minutes. It was then centrifuged at 3,500 rpm for 20 minutes, and the supernatant was
158 discarded. Then, 100 µL of 0.3% NBT in Hank's Buffered Salt Solution (HBSS) was
159 added and left at room temperature for 2 hours. The mixture was centrifuged again at
160 3,500 rpm for 10 minutes, the supernatant was discarded, and 100 µL of absolute
161 methanol was added. The pellet was washed twice with 70% methanol. Finally, 120 µL
162 of KOH (2M) and 140 µL of dimethyl sulfoxide (DMSO) were added to dissolve the
163 pellet. The dissolved pellet was transferred to a microplate to measure the optical density
164 (OD) using a microplate reader at 630 nm (Cheng et al. 2004).

165 Prophenoloxidase (PO) activity in hemocytes was measured based on the
166 formation of dopachrome produced by L-dihydroxyphenylalanine (L-DOPA). A total of
167 1 mL of the hemolymph-anticoagulant mixture was centrifuged at 3,500 rpm for 10
168 minutes at 4°C. The supernatant was discarded, and the pellet was slowly resuspended
169 with 1 mL of cacodylate-citrate buffer (0.01 M sodium cacodylate, 0.45 M sodium
170 chloride, 0.10 M trisodium citrate, pH 7). The mixture was centrifuged again at 3,500 rpm
171 for 10 minutes at 4°C. After discarding the supernatant, 200 µL of cacodylate buffer was
172 added. A 100 µL cell suspension was incubated with 50 µL trypsin (1 mg/mL in
173 cacodylate buffer) as an activator for 10 minutes at 25-26°C. Then, 50 µL L-DOPA (3
174 mg/mL in cacodylate buffer) was added and left for 5 minutes before adding 800 µL of
175 cacodylate buffer. A 200 µL suspension was transferred to a microplate, and OD was
176 measured using a microplate reader at 490 nm (Liu and Chen 2004).

177 2.4.5 Gejala Klinis dan Pemeriksaan Histopatologi Udang Vaname

178 Clinical symptom observations were conducted throughout the pathogenicity test.
179 Shrimp were observed macroscopically post-challenge, noting the condition of the body,
180 organs, and behavioral changes (Saulnier et al., 2000).

181 Histopathological preparations were made by dissecting shrimp to collect the
182 hepatopancreas and intestines, which were preserved in Davidson's solution. The
183 histopathological procedure included fixation, dehydration, clearing, embedding,
184 sectioning, and staining. The prepared slides were examined under a microscope at
185 40x100 magnification to observe the integrity or damage of the cells in each treatment.
186 According to Izwar et al. (2018), tissue examination was conducted by observing five
187 different fields of view to ensure high accuracy in the results.

188 **2.5 Statistical Analysis**

189 The research parameter data was tabulated using Microsoft Excel 2019 software.
190 The tabulated data was then analyzed using the analysis of variance (ANOVA) method
191 with a 95% confidence interval, and if significant results were obtained, the analysis
192 would be continued using Duncan's test with IBM SPSS version 26.0 software.

193

194 **3 RESULT**

195 **3.1 *V. parahaemolyticus* and AHPND Confirmation**

196 The colony color of *V. parahaemolyticus* bacteria grown on selective media for
197 *Vibrio* sp., namely thiosulfate citrate bile salt sucrose (TCBS) and CHROMagar, showed
198 colors consistent with *V. parahaemolyticus* (Figure 1). On TCBS media, the bacterial
199 colonies appeared green, while on CHROMagar media, the colonies appeared purple. The
200 colony colors on both media corresponded to the characteristics of *V. parahaemolyticus*.
201 Furthermore, the PCR test results using the AP4 primer, a specific primer for detecting

202 AHPND, showed visualizations as presented in Figure 2. The PCR visualization results
203 indicated that both isolates tested positive for AHPND with an amplicon size of 230 bp.
204 This is evidenced by the alignment of the positive control amplicon with both samples,
205 as well as above the 200 bp marker.

206 **3.2 White Shrimp Mortality Pattern**

207 The observation results of white shrimp mortality every 12 hours are presented as
208 a cumulative mortality percentage graph (Figure 3). In the control group (K), no mortality
209 occurred during the maintenance period. In the Vp-1 treatment, most mortality occurred
210 between the 12th and 48th hours, with no further mortality observed from the 48th to the
211 168th hour. In the Vp-2 treatment, mortality began at the 12th hour and continued until
212 the end of the maintenance period at the 168th hour.

213 **3.3 Mortality and Mean Time to Death (MTD)**

214 The observations of mortality and MTD (Mean Time to Death) showed different
215 results between treatments K, Vp-1, and Vp-2 (Table 1). In treatment K, no shrimp died
216 during the maintenance period, resulting in a mortality and MTD value of 0. The highest
217 mortality and MTD were found in treatment Vp-1 at $81.67 \pm 15.28\%$, with an MTD of
218 24.28 hours. Meanwhile, treatment Vp-2 had a mortality rate of $73.33 \pm 20.21\%$ with an
219 MTD of 65.44 hours. ANOVA results for the three treatments indicated that treatment K
220 was significantly different ($P < 0.05$) from treatments Vp-1 and Vp-2.

221 **3.4 Bacterial Population**

222 The population of *V. parahaemolyticus* on TCBS and CHROMagar media showed
223 no significant difference from one another, except for treatment K (Table 2). In treatment
224 K, no bacteria grew until the end of the maintenance period on both media. Treatment
225 Vp-1 had the highest bacterial population in the water at H0 on TCBS media (4.66 ± 0.07

226 Log CFU/mL and CHROMagar (4.50 ± 0.09 Log CFU/mL). The bacterial population in
227 the water continued to decrease daily until H7. The ANOVA results for treatment Vp-1
228 regarding the bacterial population in the water on TCBS and CHROMagar indicated no
229 significant difference. The highest bacterial population for Vp-1 on the shrimp body was
230 at H1 on TCBS media (4.29 ± 0.50 Log CFU/g) and CHROMagar (4.01 ± 0.53 Log CFU/g).
231 The ANOVA results for treatment Vp-1 regarding the bacterial population on the body
232 on TCBS and CHROMagar showed no significant difference. Treatment Vp-2 had the
233 highest bacterial population in the water at H0 on TCBS media (4.95 ± 0.44 Log CFU/mL)
234 and CHROMagar (4.74 ± 0.35 Log CFU/mL). The bacterial population for Vp-2 in the
235 water continued to decrease until H7. The ANOVA results for treatment Vp-1 regarding
236 the bacterial population in the water on TCBS and CHROMagar indicated no significant
237 difference. The highest bacterial population for Vp-2 on the body was at H1 on TCBS
238 media ($4.35 \pm 1.05a$ Log CFU/g) and CHROMagar (4.08 ± 0.92 Log CFU/g), and it
239 continued to decrease until H7. The ANOVA results for treatment Vp-1 regarding the
240 bacterial population on the body on TCBS and CHROMagar showed no significant
241 difference.

242 **3.5 White Shrimp Immune Response**

243 The results of the total haemocyte count (THC) measurements for all treatments
244 are presented in Figure 4. The THC of white shrimp in treatment K had the highest value
245 ($4.58 \pm 0.55 \times 10^4$ CFU/mL), while the lowest value was found in treatment Vp-2
246 ($2.22 \pm 0.76 \times 10^4$ CFU/mL). The ANOVA results for the three treatments showed that
247 treatment K was significantly different ($P < 0.05$) from treatments Vp-1 and Vp-2.

248 The data for the measurements of phagocytic activity (AF) for each treatment can
249 be seen in Figure 5. AF in treatment Vp-1 had the highest value ($74.67 \pm 4.04\%$), while

250 the lowest value was observed in treatment K ($64\pm 3.00\%$). The ANOVA results for the
251 three treatments showed that treatment K was significantly different ($P<0.05$) from
252 treatments Vp-1 and Vp-2.

253 The values for the respiratory burst (RB) in each treatment showed different
254 numbers (Figure 6). RB in treatment K had the highest value (1.08 ± 0.12), while the
255 lowest value was found in treatment Vp-2 (0.63 ± 0.06). The ANOVA results for the three
256 treatments indicated that treatments K and Vp-1 were significantly different ($P<0.05$)
257 from treatment Vp-2.

258 The results of the phenoloxidase activity measurements can be seen in Figure 7.
259 PO in treatment K had the highest value (0.13 ± 0.01), while the lowest value was found
260 in treatment Vp-1 (0.08 ± 0.02). The ANOVA results for the three treatments showed that
261 treatment K was significantly different ($P<0.05$) from treatments Vp-1 and Vp-2.

262 **3.6 White Shrimp Clinical Symptoms**

263 Clinical symptoms caused by *V. parahaemolyticus* infection during rearing can be
264 seen in Figure 8. The movement of white shrimp in treatments Vp-1 and Vp-2 at 12 hours
265 after the challenge test started showed weakness, swimming in a tilted or unbalanced
266 manner. The shrimp were also seen at the bottom of the aquarium with minimal
267 movement. Macroscopic observations of the bodies in both treatments showed that the
268 shrimp appeared pale, with the hepatopancreas appearing whitish and the intestines
269 appearing empty. Meanwhile, in the control treatment (K), there were no changes during
270 the treatment. Macroscopic observations of the control treatment showed that the shrimp's
271 body appeared bluish-clear, with the hepatopancreas reddish in color, and the intestines
272 appeared full.

273 **3.7 White Shrimp Histopathology**

274 Histopathological observations of the hepatopancreas showed differences
275 between the control treatment (K) and treatments Vp-1 and Vp-2 (Figure 9). The control
276 treatment showed many normal tubules and normal cells. In treatment Vp-1, there was
277 noticeable necrosis of B cells and numerous vacuoles. Necrotic tubules were commonly
278 found, appearing shattered and shapeless. Treatment Vp-2 also exhibited similar damage,
279 including significant necrosis and vacuoles, with many damaged tubules observed. The
280 tissue in the control treatment appeared more stained compared to treatments Vp-1 and
281 Vp-2.

282 Histopathological observations of the intestines revealed differences between the
283 control treatment (K) and treatments Vp-1 and Vp-2 (Figure 3). The tissue in infected
284 shrimp (Vp-1 and Vp-2) exhibited massive damage or necrosis of the intestinal wall, with
285 numerous B cell necroses also present in both treatments. Inflammation or inflammatory
286 cells were found at several points. Meanwhile, in the uninfected treatment (K), the
287 intestinal wall tissue was intact with a regular lumen. Necrosis and tissue inflammation
288 were not found in this treatment.

289

290 **4 DISCUSSION**

291 The role of a microbe in attacking a host to cause a disease is called pathogenesis
292 (Amrullah 2014). Certain strains of *V. parahaemolyticus* are the cause of acute
293 hepatopancreatic necrosis disease (AHPND). Testing was conducted by observing the
294 pathogenicity level of the bacteria against white shrimp. Characterization tests for *V.*
295 *parahaemolyticus* were performed on TCBS and CHROMagar media. TCBS media is
296 specific for *Vibrio* sp., while CHROMagar is specific for *V. parahaemolyticus*, *V.*
297 *vulnificus*, *V. cholerae*, and *V. alginolyticus*. Both media contain specific compositions to

298 inhibit the growth of non-target bacteria. Bacteria grown on TCBS media show green-
299 colored colonies. *Vibrio* sp. that cannot ferment sucrose in TCBS media, such as *V.*
300 *parahaemolyticus* and *V. vulnificus*, will produce green colonies, while those that can
301 ferment sucrose, like *V. cholerae* and *V. alginolyticus*, have yellow colonies (Lee et al.
302 2020). Meanwhile, on CHROMagar, the bacterial colonies appear purple. According to
303 Lee et al. (2020), *V. vulnificus* and *V. cholerae* have blue colonies, while *V. alginolyticus*
304 appears yellowish-white, and *V. parahaemolyticus* has purple colonies. A confirmation
305 test for AHPND was then conducted using the Polymerase Chain Reaction (PCR)
306 method.

307 The AHPND testing was performed with two PCR steps: first-step PCR and
308 nested PCR. According to Hoang et al. (2021), nested PCR is performed to obtain high-
309 accuracy amplicons that match the target. Positive and negative controls were used as
310 comparisons for sample results. The main stages included DNA extraction, amplification,
311 and electrophoresis, followed by visualization of the PCR results. The visualization of the
312 PCR electrophoresis results showed that the bacteria Vp-1 and Vp-2 tested positive for
313 AHPND with DNA bands measuring 230 bp. This aligns with Dangtip et al. (2015),
314 which states that *V. parahaemolyticus* is considered positive for AHPND if it has a DNA
315 band measuring 1269 bp in first-step PCR and 230 bp in nested PCR.

316 Shrimp infected by *V. parahaemolyticus*, the cause of AHPND, will experience
317 early mortality. The disease previously known as Early Mortality Syndrome typically
318 causes deaths in shrimp farms during the early months of rearing, before DOC-35
319 (Rodriguez et al. 2019). The mortality pattern shows the cumulative mortality percentage
320 over time (Figure 3). The highest percentage of mortality in treatments Vp-1 and Vp-2
321 occurs from hour 12 to hour 24. A drastic increase in mortality at hour 24 occurs in

322 treatment Vp-1, where the mortality percentage exceeds 50% of the population.
323 Treatment Vp-1 shows the highest mortality percentage ($81.67 \pm 15.28b$) with the fastest
324 average time to death (ATD), while mortality in treatment Vp-2 has a lower percentage
325 and a slower ATD compared to Vp-1. According to Hong et al. (2016), vannamei shrimp
326 infected with AHPND have mortality rates ranging from 40% to 100%.

327 The bacterial population in the water in the challenge treatments (Vp-1 and Vp-2)
328 has the highest density on day 0 and continues to decline until the end of the observation.
329 According to Valente and Wan (2021), bacteria that do not find a host will die because
330 they do not receive nutrients to survive. This shows that the bacterial density in the water
331 continues to decrease due to the declining or even absent population of vannamei shrimp
332 as hosts. The bacterial population on the shrimp bodies also decreases daily. This can be
333 linked to the decreasing number of bacteria in the water, leading to fewer bacteria entering
334 the shrimp's body.

335 The results of measuring total hemocyte count (THC) after the challenge test
336 showed that the control treatment (K) had the highest value. Hemocytes play an important
337 role in crustaceans as they help eliminate or compete with foreign particles entering the
338 crustacean body, such as disease-causing pathogens (Hauton 2012). According to Sahoo
339 et al. (2007), hemocytes can act as a cellular defense system in white shrimp, playing a
340 role in phagocytosis, encapsulation, and nodulation. The number of hemocytes in the
341 shrimp body can influence the infection level of *V. parahaemolyticus*. The more
342 hemocytes present, the lower the infection level. This can affect the survival rate of
343 vannamei shrimp after the challenge test. Treatment Vp-2 had the lowest THC value;
344 according to Smith et al. (2003), low THC values indicate a defense mechanism occurring
345 during pathogen infection. The decrease in THC is due to hemocytes migrating to the

346 infected tissues, thus affecting immune response performance at that site (Hamsah et al.
347 2019).

348 Phagocytic activity showed a significant difference ($P < 0.05$) between treatment
349 K and treatments Vp-1 and Vp-2. Phagocytic activity plays a role in the immune response
350 mechanism of vannamei shrimp against pathogen infections and physiological processes
351 such as tissue repair (Liu et al. 2020). Hemocytes are the cells involved in the
352 phagocytosis process to combat various pathogens, including *V. parahaemolyticus*, to
353 protect their hosts. The highest phagocytic activity value is found in treatment Vp-1,
354 followed by Vp-2, while K has the lowest phagocytic value. According to Braak (2002),
355 there are three types of hemocyte cells: hyaline, granular, and semi-granular. Hyaline
356 cells play a role in phagocytic activity, while semi-granular cells function as temporary
357 phagocytic cells. An increase in THC value can enhance phagocytic activity (Johansson
358 et al. 2000).

359 Respiratory burst (RB) is part of the shrimp's immune response system against
360 pathogen infections. White shrimp infected by pathogens like viruses or bacteria will
361 respond through hemocytes with increased reactive oxygen production. This process is
362 marked by the reduction of nitroblue tetrazolium (NBT) by hemocytes. RB is a
363 continuation of phagocytosis, and the two processes are interconnected because the
364 digestive enzymes of RB are bactericidal agents that are released from the
365 phagolysosome, resulting in free radical release from the phagolysosome (Risjani et al.
366 2021). The RB results in the study showed that treatment K had the highest value, while
367 Vp-2 had the lowest value. The assumption that treatment Vp-1 has a lower value than
368 Vp-2 is due to the lower mortality rate in Vp-1. This is likely because sampling was
369 conducted simultaneously at hour 24 across all treatments. It is assumed that treatment

370 Vp-1 reached its peak mortality before hour 24, so at the time of sampling, it was already
371 in the recovery phase. According to Wang et al. (2012), the post-disease attack recovery
372 process in vannamei shrimp can enhance RB values.

373 Phenoloxidase (PO) in shrimp plays a role in biological functions such as defense
374 against pathogens, wound healing, and body color regulation. The mechanism of PO
375 begins with phenol oxidase, forming quinone that generates dark brown pigments to
376 inactivate and prevent pathogens. This process is called melanization (Amparyup et al.
377 2013). The measurement of PO in the challenged treatments (Vp-1 and Vp-2) showed
378 lower values compared to the control treatment without challenge (K). According to Costa
379 et al. (2009), a decrease in the immunity level or defense of shrimp will lower PO activity,
380 while shrimp with good immunity will have high PO values.

381 Shrimp infected with AHPND exhibit lethargic movement, anorexia, slow
382 growth, empty digestive tracts, and pale to white hepatopancreas (Kumar et al. 2021).
383 The clinical symptoms exhibited in the infected treatments (Vp-1 and Vp-2) have similar
384 characteristics. The shrimp's body appears pale, the carapace softens, and slowed
385 movement is observed, with their bodies appearing unbalanced or tilted at the bottom.
386 Internal organ attacks on the hepatopancreas show a pale white color, and the intestines
387 are empty. Meanwhile, in the uninfected treatment (K), no symptoms are observed. The
388 shrimp's body is bluish-clear, with active movement, reddish-brown hepatopancreas, and
389 filled intestines. According to Nunan et al. (2014), healthy vannamei shrimp have a bright
390 clear body color, are actively moving, and have reddish-brown hepatopancreas, with full
391 intestines displaying an unbroken black line.

392 Histopathology is performed to observe pathological changes at the microscopic
393 level in shrimp tissues. The pathogen's ability to infect a host can affect tissues at the

394 microscopic level. Tissues can suffer acute damage due to pathogen attacks, such as
395 viruses or bacteria. *V. parahaemolyticus*, which causes AHPND, attacks the
396 hepatopancreas and intestines with acute damage levels (Suryana et al. 2023). The
397 hepatopancreas tissue in shrimp infected with AHPND shows high levels

398

399 **5 CONCLUSION**

400 Isolates Vp-1 and Vp-2 were identified as *V. parahaemolyticus* strains causing
401 AHPND that infect Pacific white shrimp, presenting clinical symptoms such as pale
402 hepatopancreas, empty intestines, and reduced activity. Tissue damage was evident with
403 significant necrosis in the hepatopancreas and intestinal organs, resulting in mortality
404 rates ranging from 73.33% to 81.67%, with an average time to death of 24.28 to 65.44
405 hours.

406

407 **CONFLICT OF INTEREST**

408 We declare that there are no conflicts of interest regarding financial, personal, or
409 other relationships with individuals or organizations related to the material discussed in
410 the manuscript.

411

412 **ACKNOWLEDGEMENT**

413 Thank you to PT. Agrinusa Jaya Santosa for supporting this research activity

414

415 **REFERENCES**

- 416 **Abdel-Latif, H. M., E. Yilmaz, M. A. Dawood, E. Ringø, E. Ahmadifar, & S. Yilmaz.**
417 2022. Shrimp vibriosis and possible control measures using probiotics,
418 postbiotics, prebiotics, and synbiotics: A review. *Aquaculture*. 551: 1-23.
- 419 **Aguirre-Guzmán, G., J. G. Sánchez-Martínez, R. Pérez-Castañeda, A. Palacios-**
420 **Monzón, T. Trujillo-Rodríguez, & N. I. dela Cruz-Hernández.** 2010.
421 Pathogenicity and infection route of *Vibrio parahaemolyticus* in American white
422 shrimp, *Litopenaeus vannamei*. *J. World Aquac. Soc.* 41(3): 464-470.
- 423 **Amparyup, P., Charoensapsri, W., & Tassanakajon, A.** 2013. Prophenoloxidase
424 system and its role in shrimp immune responses against major pathogens. *Fish.*
425 *Shellfish. Immunol.* 34(4): 990-1001.
- 426 **Anderson, D. P., & A. K. Siwicki.** 1993. Basic haematology and serology for fish health
427 programs. Paper Presented in Second Symposium on Diseases in Asia
428 Aquaculture “Aquatic Animal Health and The Environmental”. Phuket, Thailand.
429 25-29th October 1993.
- 430 **Amrullah.** 2014. Immunoproteksi vaksin toksid bakteri *Streptococcus agalactiae* pada
431 ikan nila (*Oreochromis niloticus*) [Disertasi]. Bogor (ID): Sekolah Pasca Sarjana,
432 Institut Pertanian Bogor.
- 433 **Braak, K. V. D.** 2002. Haemocytic defence in black tiger shrimp (*Penaeus monodon*)
434 [Disertasi]. Wageningen (NL): Wageningen Institute of Animal Science.
- 435 **Cheng, W., C. H. Liu, S. T. Yeh, & J. C. Chen.** 2004. The immune stimulatory effect
436 of sodium alginate on the white shrimp *Litopenaeus vannamei* and its resistance
437 against *Vibrio alginolyticus*. *Fish Shellfish Immunol.* 17: 41-51.

- 438 **Costa, A. M., C. C. Buglione, F. L. Bezerra, P. C. C. Martins, & M. A. Barracco.**
439 2009. Immune assessment of farm-reared *Penaeus vannamei* shrimp naturally
440 infected by IMNV in NE Brazil. *Aquaculture*. 291: 141-146.
- 441 **Dangtip, S., R. Sirikharin, P. Sanguanrut, S. Thitamadee, K. Sritunyalucksana, S.**
442 **Taengchaiyaphum, R. Mavichak, & T. W. Flegel.** 2015. AP4 method for two-
443 tube nested PCR detection of AHPND isolates of *Vibrio parahaemolyticus*.
444 *Aquaculture Reports*. 2(1): 158-162.
- 445 **Effendi, M. I.** 1997. *Biologi Perikanan*. Bogor (ID): Yayasan Pustaka Nusantara.
- 446 **[FAO] Food and Agriculture Organization of the United Nations.** 2022. The State of
447 World Fisheries and Aquaculture 2022 [Internet]. [Accessed 2023 Aug
448 6]; <http://www.fao.org/fishery/statistics>.
- 449 **Hamsah, H., W. Widanarni, A. Alimuddin, M. Yuhana, M. Z. Junior, & D.**
450 **Hidayatullah.** 2019. Immune response and resistance of Pacific white shrimp
451 larvae administered probiotic, prebiotic, and synbiotic through the
452 bioencapsulation of *Artemia* sp. *Aquac. Int.* 27(2): 1-14.
- 453 **Han, J. E., Tang, K. F., Tran, L. H., & Lightner, D. V.** 2015. Photorhabdus insect-
454 related (Pir) toxin-like genes in a plasmid of *Vibrio parahaemolyticus*, the
455 causative agent of acute hepatopancreatic necrosis disease (AHPND) of
456 shrimp. *Dis. Aquat. Org.* 113(1): 33-40.
- 457 **Hauton, C.** 2012. The scope of the crustacean immune system for disease control. *J.*
458 *Invert. Pathol.* 110(2): 251-260.
- 459 **Hoang, T. D. M., H. L. Tien, H. H. M. C. Hoang, K. H. N. Phuoc, H. Q. Pham, T. L.**
460 **Tran, & H. T. Van.** 2021. A novel PCR method for simultaneously detecting

- 461 acute hepatopancreatic necrosis disease (AHPND) and mutant-AHPND in shrimp.
462 Aquaculture. 534: 1-7.
- 463 **Hong, X., L. Lu, & D. Xu.** 2016. Progress in research on acute hepatopancreatic necrosis
464 disease (AHPND). Aquac. Int. 24: 577-593.
- 465 **Izwar, A.** 2018. Isolasi, identifikasi, dan uji patogenisitas bakteri penyebab penyakit pada
466 ikan kakap putih Lates calcarifer [Tesis]. Bogor (ID): Institut Pertanian Bogor.
- 467 **Johansson, M. W., P. Keyser, K. Sritunyaluksana, & K. Soderhall.** 2000. Crustacean
468 haemocytes and haematopoiesis. Aquaculture. 191: 45-52.
- 469 **[KKP] Kementerian Kelautan dan Perikanan.** 2022. Kelautan dan Perikanan Dalam
470 Angka Tahun 2022. Jakarta (ID): Kementerian Kelautan dan Perikanan.
- 471 **Kumar, V., S. Roy, B. Behera, P. Bossier, & B. K. Das.** 2021. Acute hepatopancreatic
472 necrosis disease (AHPND): virulence, pathogenesis and mitigation strategies in
473 shrimp aquaculture. Toxins. 13(8): 1-28.
- 474 **Lee, J. M., R. N. Azizah, & K. S. Kim.** 2020. Comparative evaluation of three agar
475 media-based methods for presumptive identification of seafood-originated *Vibrio*
476 *parahaemolyticus* strains. Food Control. 116: 1-6.
- 477 **Liu, C. H., & J. C. Chen.** 2004. Effect of ammonia on the immune response of white
478 shrimp *Litopenaeus vannamei* and its susceptibility to *Vibrio alginolyticus*. Fish
479 Shellfish Immunol. 16: 321-324.
- 480 **Liu, S., Zheng, S. C., Li, Y. L., Li, J., & Liu, H. P.** 2020. Hemocyte-mediated
481 phagocytosis in crustaceans. Front. Immunol. 11: 268.
- 482 **Madigan, M. T., J. Martinko, & J. B. Parker.** 2003. The Biology of Microorganisms.
483 New Jersey (US): Prentice Hall.

- 484 **Muharrama, A. R. W., W. Widanarni, A. Alimuddin, & M. Yuhana.** 2021. Gene
485 expression and immune response of Pacific white shrimp given *Bacillus* NP5
486 probiotic and honey prebiotic and *Vibrio parahaemolyticus* infection. *J. Appl.*
487 *Aquac.* 34(3): 1-17.
- 488 **Nazaruddin, D. Aliza, S. Aisyah, Zainuddin, & Syafrizal.** 2014. Gambaran
489 histopatologis hepatopankreas udang windu (*Penaeus monodon*) akibat infeksi
490 virus hepatopancreatica parvovirus (HPV). *J. Kedokteran Hewan.* 8(1): 27-29.
- 491 **Nitimulyo, K. H., A. Isnansetyo, Triyanto, M. Murdjani, & L. Sholchah.** 2005.
492 Efektivitas vaksin polivalen untuk pengendalian vibriosis pada kerapu tikus
493 (*Cromileptes altivelis*). *J. Perikanan.* 7(2): 95-100.
- 494 **Nunan, L., D. Lighner, C. Pantoja, & S. Gomez-Jimenez.** 2014. Detection of acute
495 hepatopancreatic necrosis disease (AHPND) in Mexico. *Dis. Aquatic Organ.*
496 111(1): 81-86.
- 497 **[OIE] Office International des Epizooties.** 2019. Manual of Diagnostic Tests for
498 Aquatic Animals. Chapter 2.2.1. OIDE: France.
- 499 **Risjani, Y., N. Mutmainnah, P. Manurung, S. N. Wulan, & Yunianta.** 2021.
500 Exopolysaccharide from *Porphyridium cruentum* (purpureum) is not toxic and
501 stimulates immune response against vibriosis: the assessment using zebrafish and
502 white shrimp *Litopenaeus vannamei*. *Mar. Drugs.* 19(133): 1-17.
- 503 **Rodriguez, S., O. R. Lozano, P. Gonzales, M. D. A. Bolan, & R. Anguilar.** 2019.
504 Characterization and growth conditions of *Vibrio parahaemolyticus* strains with
505 different virulence degrees that cause acute hepatopancreatic necrosis disease in
506 *Litopenaeus vannamei*. *J. World Aquac. Soc.* 50(5): 1002-1015.

- 507 **Sahoo, P. K., B. R. Pillai, J. Mohanty, J. Kumari, S. Mohanty, & B. K. Mishra.** 2007.
508 In vivo humoral and cellular reaction, and fate of injected bacteria *Aeromonas*
509 *hydrophila* in freshwater prawn *Macrobrachium rosenbergii*. *Fish Shellfish*
510 *Immunol.* 23: 327-340.
- 511 **Saulnier, D., Haffner, P., Goarant, C., Levy, P., & Ansquer, D.** 2000. Experimental
512 infection models for shrimp vibriosis studies: a review. *Aquaculture*, 191(1-3):
513 133-144.
- 514 **Smith, V. J., J. H. Brown, & C. Hauton.** 2003. Immunostimulation in crustaceans: does
515 it really protect against infection?. *Fish Shellfish Immunol.* 15(1): 71.
- 516 **Takeuchi.** 2003. *Role of COX inhibition in pathogenesis of NSAID-induced small*
517 *intestinal damage.* Kyoto (JP): Kyoto Pharmaceutical University.
- 518 **Tang, K. F. J., & Bondad-Reantaso, M. G.** 2019. Impacts of acute hepatopancreatic
519 necrosis disease on commercial shrimp aquaculture. *Rev. Sci. Tech.* 38: 477-490.
- 520 **Tran, L., Nunan, L., Redman, R. M., Mohny, L. L., Pantoja, C. R., Fitzsimmons,**
521 **K., & Lightner, D. V.** 2013. Determination of the infectious nature of the agent
522 of acute hepatopancreatic necrosis syndrome affecting penaeid shrimp. *Dis.*
523 *Aquat. Org.* 105(1): 45-55.
- 524 **Valente, C. D. S., & Wan, A. H.** 2021. *Vibrio* and major commercially important
525 vibriosis diseases in decapod crustaceans. *J. Invertebr Pathol.* 181: 107527.
- 526 **Widanarni, W., Gustilatov, M., Ekasari, J., Julyantoro, P. G. S., Waturangi, D. E.,**
527 **& Sukenda, S.** 2024. Unveiling the positive impact of biofloc culture on *Vibrio*
528 *parahaemolyticus* infection of Pacific white shrimp by reducing quorum sensing
529 and virulence gene expression and enhancing immunity. *J. Fish. Dis.* 47(6),
530 e13932.

- 531 **Zorriehzahra, M. J., & Banaederakhshan, R. J. A. A. V. S.** 2015. Early mortality
532 syndrome (EMS) as new emerging threat in shrimp industry. *Adv. Anim. Vet.*
533 *Sci.* 3(2S): 64-72.
534
535

Accepted Manuscript

536

537 Table 1 Mortality and mean time of death (MTD) of white shrimp infected with *V.*
 538 *parahaemolyticus*

Treatment	Mortality (%)	MTD (Hours)
K	0 ^a	0
Vp-1	81,67±15,28 ^b	24,28
Vp-2	73,33±20,21 ^b	65,44

539 Note: Different letters in the same column indicate significantly different results (Duncan P<0.05)

540

541 Table 2 Population of *V. parahaemolyticus* in the water and the bodies of white shrimp
 542 infected with *V. parahaemolyticus*

Sources	Time	K		Vp-1		Vp-2	
		TCBS	CHROM	TCBS	CHROM	TCBS	CHROM
Water (Log CFU/mL)	H0	0	0	4,66±0,07 ^a	4,50±0,09 ^a	4,95±0,44 ^a	4,74±0,35 ^a
	H1	0	0	4,44±0,04 ^a	4,32±0,03 ^a	4,63±0,52 ^a	4,35±0,29 ^a
	H2	0	0	4,09±0,53 ^a	3,85±0,56 ^a	4,09±0,47 ^a	3,92±0,45 ^a
	H4	0	0	3,19±1,02 ^a	2,83±0,67 ^a	3,69±0,09 ^a	3,48±0,09 ^a
	H7	0	0	2,73±0,51 ^a	2,50±0,35 ^a	2,66±0,32 ^a	2,60±0,30 ^a
Body (Log CFU/g)	H1	-	-	4,29±0,50 ^a	4,01±0,53 ^a	4,35±1,05 ^a	4,08±0,92 ^a
	H2	-	-	2,30±1,02 ^a	2,30±0,48 ^a	4,17±1,02 ^a	3,70±0,67 ^a
	H3	-	-	-	-	3,54±0,59 ^a	3,29±0,49 ^a
	H4	-	-	-	-	3,13±0,72 ^a	2,89±0,53 ^a
	H7	-	-	-	-	2,95±0,57 ^a	2,53±0,40 ^a

543 Note: (-): No shrimp died. Different letters in the same row indicate significantly different results (Duncan
 544 P<0.05)

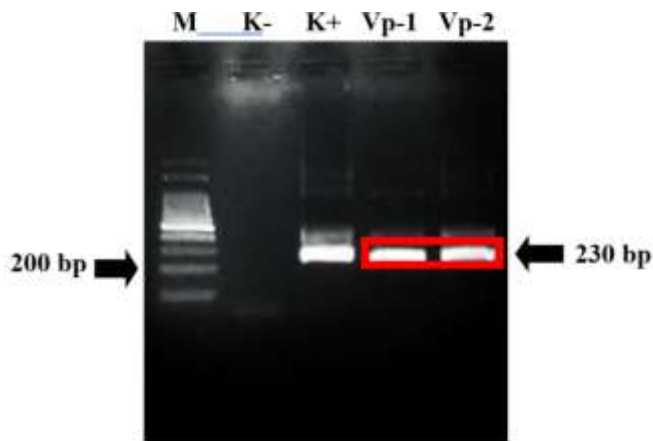
545

546

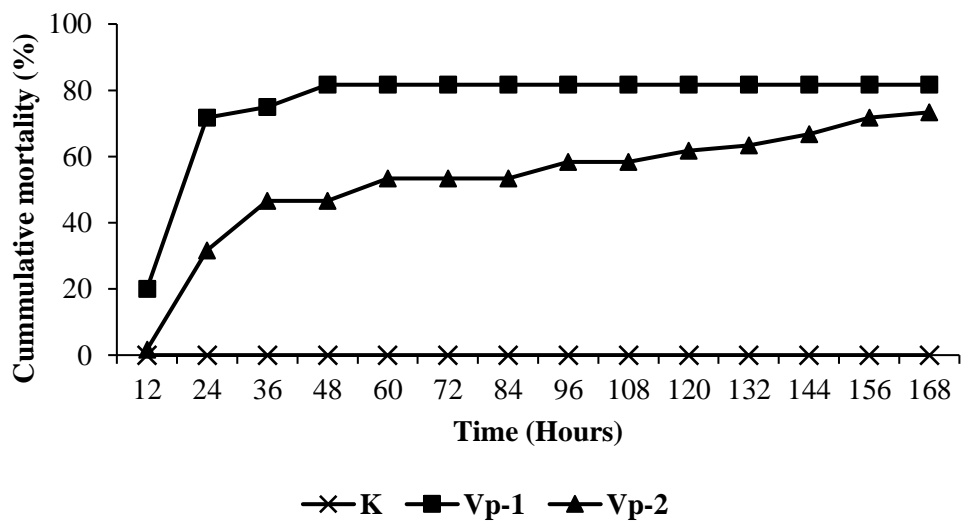
547



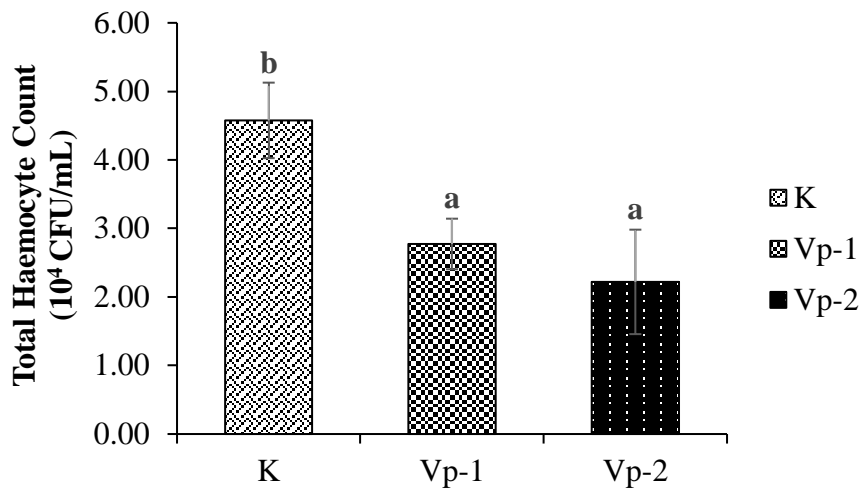
548
549 Figure 1 Colonies of *V. parahaemolyticus* on TCBS and CHROMagar media
550



551
552 Figure 2 Visualization of *V. parahaemolyticus* bacteria PCR using primer AP4
553 Note: M: marker; K-: Negative control; K+: Positive control; Vp-1: Treatment bacteria Vp-1; Vp-2:
554 Treatment bacteria Vp-2

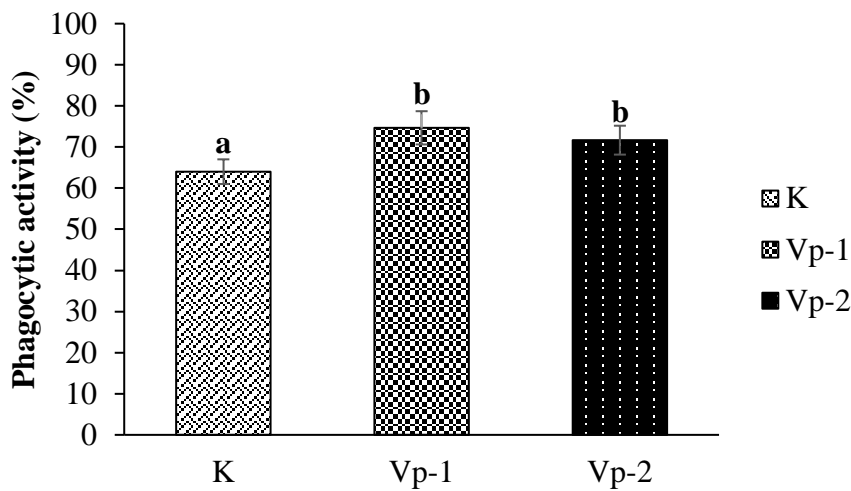


556
557 Figure 3 Cumulative mortality of white shrimp infected with *V. parahaemolyticus*



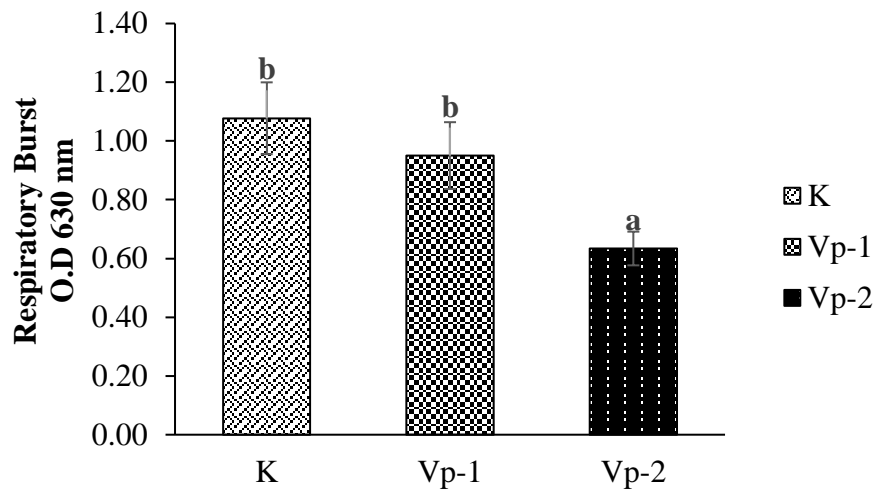
558

559 Figure 3 Total hemocyte count of white shrimp infected with *V. parahaemolyticus*
560 Note: Different letters above the bars indicate significantly different results (Duncan P<0.05)



561

562 Figure 4 Phagocytic activity of white shrimp infected with *V. parahaemolyticus*
563 Note: Different letters above the bars indicate significantly different results (Duncan P<0.05).

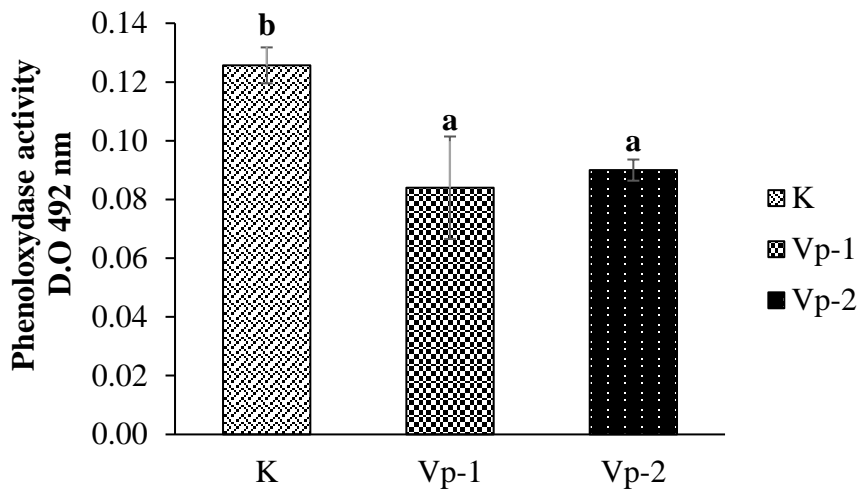


564

565 Gambar 5 Respiratory burst of white shrimp infected with *V. parahaemolyticus*

566 Note: Different letters above the bars indicate significantly different results (Duncan $P < 0.05$).

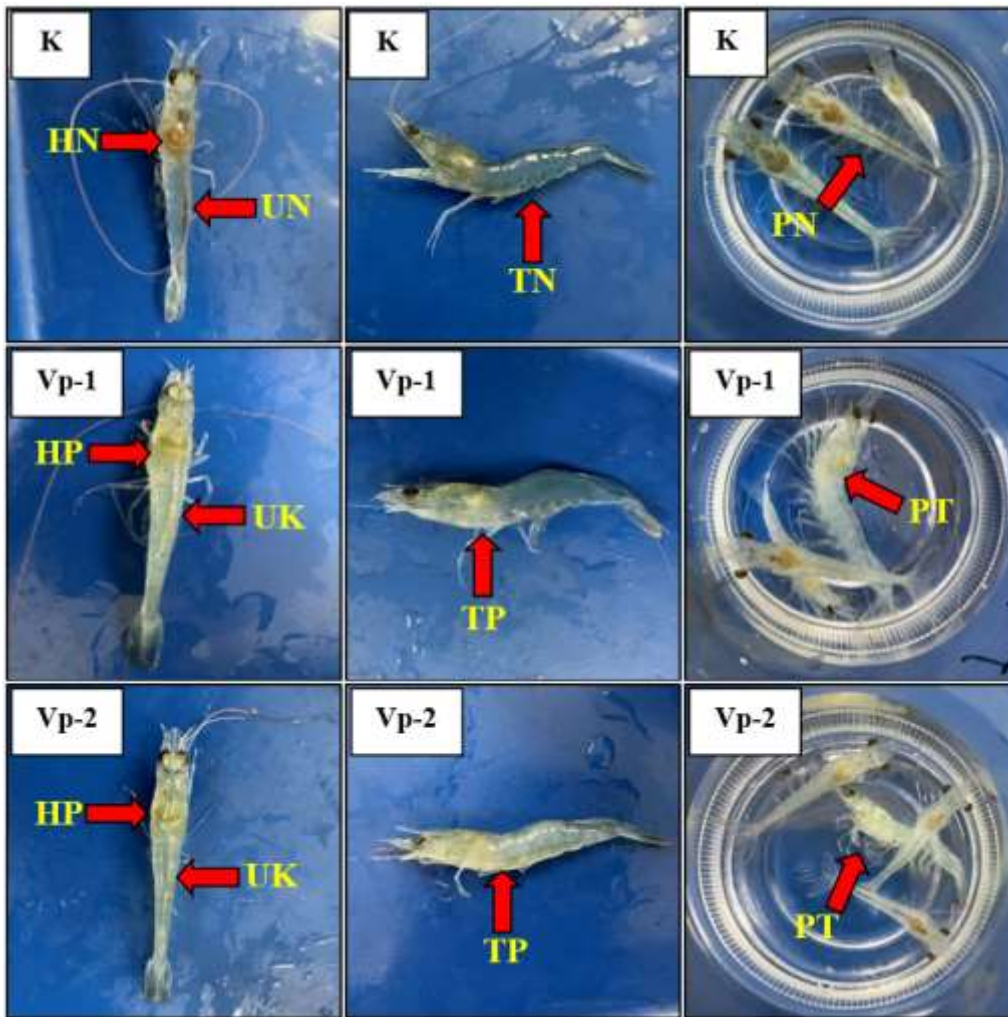
567



568

569 Figure 7 Phenoloxidase activity of white shrimp infected with *V. parahaemolyticus*

570 Note: Different letters above the bars indicate significantly different results (Duncan $P < 0.05$).

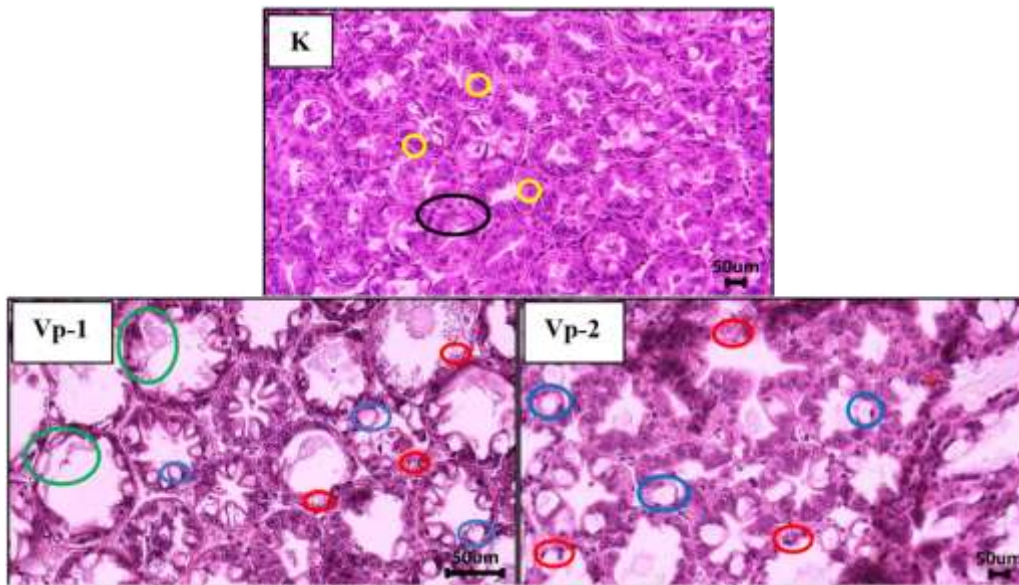


571

572 Figure 8 Clinical symptoms of white shrimp infected with *V. parahaemolyticus*

573 Note: TN: normal body; HN: normal hepatopancreas; UN: normal intestine; PN: normal movement; TP:
574 pale body; HP: pale hepatopancreas; UK: empty intestine; PT: abnormal movement. K: Vannamei shrimp
575 not infected with *V. parahaemolyticus*; Vp-1: Vannamei shrimp infected with *V. parahaemolyticus* from
576 Tasikmalaya; Vp-2: Vannamei shrimp infected with *V. parahaemolyticus* from Situbondo.

577

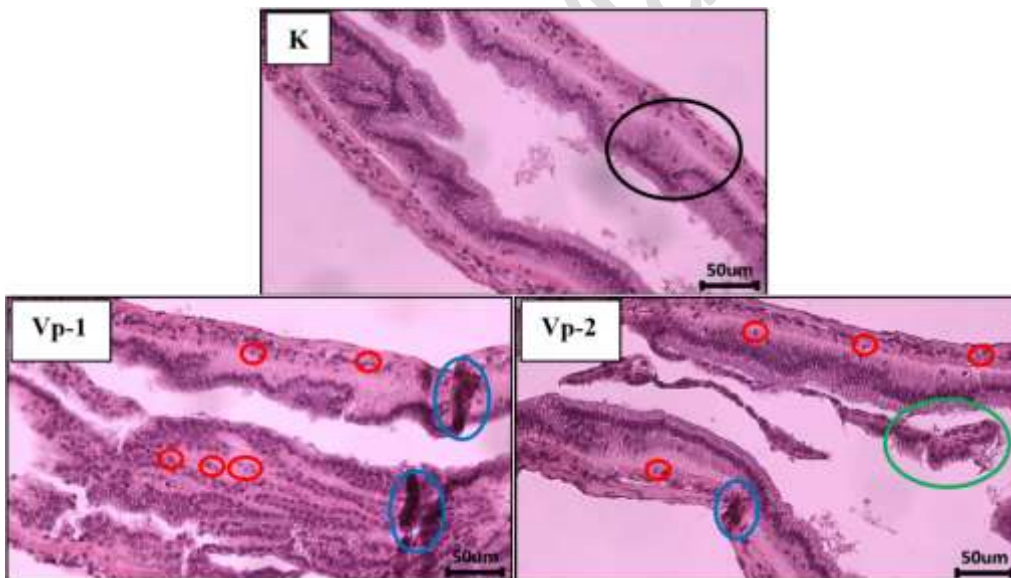


578

579 Figure 9: Histopathology of the hepatopancreas of white shrimp infected with *V.*
580 *parahaemolyticus*

581 Note: Normal tubule (○), normal cell (●), necrosis cell (●), vacuola (●), necrosis tubule (●).

582



583

584 Figure 10 Histopathology of the intestine of white shrimp infected with *V.*
585 *parahaemolyticus*

586 Note: Normal intestine wall (○), inflammation (●), intestinal wall necrosis (●), Cell necrosis (●).